Proceedings of the 28th IEEE
EMBS Annual International Conference
New York City, USA, Aug 30-Sept 3, 2006

Optical coherence tomography using rapidly swept lasers

S. H. (Andy) Yun

Abstract—**Optical coherence tomography (OCT) has proven to be a useful diagnostic tool in several medical areas. An emerging second-generation OCT technology, termed optical frequency domain imaging, is expected to increase the clinical applications of OCT significantly.**

INTRODUCTION

Optical coherence tomography (OCT) allows minimally-invasive cross-sectional imaging of biological samples [1] and has been investigated for numerous applications in biology and medicine. In most OCT systems, depth ranging is provided by low-coherence interferometry [2, 3] in which the optical path length difference between the interferometer reference and sample arms is scanned linearly in time. This embodiment of OCT, referred to as 'time-domain OCT', has demonstrated promising results for early detection of disease [4-8]. The relatively slow imaging speed (approximately 2 kHz A-line rate) of time-domain OCT systems, however, has precluded its use for screening of large tissue volumes, which is required for a wide variety of medical applications. Imaging speed has a fundamental significance because of its relationship to detection sensitivity defined as the minimum detectable reflectivity. As the A-line rate increases, the detection bandwidth should be increased proportionally, and therefore the sensitivity drops [4]. Most biomedical applications cannot tolerate a reduction in sensitivity to achieve a higher frame rate. Although increasing the optical power would, in principle, improve the sensitivity, available sources and maximum permissible exposure levels of tissue represent significant practical limitations.

One potential solution to high-speed imaging is offered by spectral-domain OCT, also known as Fourier domain OCT or spectral radar, where individual spectral components of low coherence light are detected separately by use of a spectrometer and a charge-coupled device array [9, 10]. The fast readout speed of the array and the signal-to-noise advantage of the spectral-domain OCT [11, 12] make it promising for some high-speed and low-power applications.

Optical frequency domain imaging (OFDI), also known as swept source OCT, is a new method that uses a wavelength-swept light source to probe the amplitude and phase of back scattering light from tissue [13-15]. OFDI is based on coherent optical frequency domain reflectometry (OFDR), a well-known ranging method initially developed for the measurement of depth-resolved back-reflection along optical fibers or inside optical components [16-18]. The axial profile is obtained in the electrical frequency domain by using a frequency (wavelength) swept light source. One-dimensional OFDR has also been applied to the measurement of axial intraocular dimensions [19, 20]. OFDI is the extension of OFDR to multidimensional acquisition, typically through the use of transverse beam scanning. Early demonstrations of OFDI [21-23] suffered from slow scanning speeds and relatively poor signal to noise ratio, recent works have demonstrated the feasibility for biomedical applications [15, 24]. With the recently developed rapidly tunable lasers in the 1300-nm range, OFDI has enabled significant improvements in imaging speed, sensitivity, and ranging depth over conventional time-domain OCT systems and been demonstrated for imaging skin, coronary artery, esophagus, and anterior eye segments [25-31].

While retinal imaging is the most established clinical use of OCT, until recently this application has been out of reach because the optical absorption in human eye at 1300 nm is too large. We have developed a high-performance wavelength-swept laser with a center wavelength at 1050 nm. Using an OFDI system employing the laser source, we demonstrated the first OFDI imaging of posterior segments of the human eye *in vivo* with high image acquisition speed, sensitivity, and penetration depth. The standard spectral range of conventional ophthalmic OCT has been between 700 and 900 nm where the humors in the eye are transparent and broadband super-luminescent-diode (SLD) light sources are readily available [32, 33]. Recent studies have suggested that the 1040-nm spectral range [34-36] could be a viable alternative operating window for retinal imaging and potentially could offer deeper penetration into the choroid below the highly absorbing and scattering retinal pigment epithelium. Spectral domain OCT using broadband light sources at 800 nm and spectrometers has been developed to enable three-dimensional retinal imaging *in vivo* with superior image acquisition speed and sensitivity to conventional time-domain OCT [37, 38]. Compared to SD-OCT, OFDI offers several advantages, such as immunity to motion-induced signal fading [39], simple polarization-sensitive or diversity scheme [25], and long ranging depth [15].

RAIDLY SWEPT LASER

Figure 1(a) depicts a schematic of the laser source. The gain medium was a commercially-available, bi-directional semiconductor optical amplifier (QPhotonics, Inc., QSOA-1050) driven at an injection current level of 400 mA. One

Manuscript received May 8, 2006. This work was supported by the National Institute of Health under Grant CA110130. Dr. Yun is with Harvard Medical School, Wellman Center for Photomedicine, Massachusetts General Hospital, 50 Blossom Street, BAR 818, Boston, MA 02114 USA. (phone: 617-724-6152; e-mail: syun@hms.harvard.edu).

port of the amplifier was coupled to a wavelength-scanning filter [40] that comprised a diffraction grating (1200 lines/mm), a telescope (f1 = 100 mm, f2 = 50 mm), and a polygon mirror scanner (Lincoln Lasers, Inc., 40 facets). The design bandwidth and free spectral range of the filter were ~0.1 nm and 61 nm, respectively. The amplifier's other port was spliced to a loop mirror made of a 50/50 coupler. The Sagnac loop also served as an output coupler. The reflectivity and output coupling ratio were complementary and optimized by adjusting a polarization controller (PC1) to tune the amount of birefringence-induced non-reciprocity in the loop. The linear-cavity configuration is an attractive alternative to the previous ring-cavity design [40] as low-loss low-cost circulators and isolators are not readily available at 1050 nm. Sweep repetition rates of up to 36 kHz were possible with 100% duty cycle, representing a significant improvement over previously demonstrated swept lasers that offered tuning rates of a few hundred Hz in the 1050-nm range and below [14]. Due to the limited sampling speed of the data acquisition board in our OFDI system described next, we operated the laser at a wavelength sweep rate of 18.8 kHz to obtain a sufficient depth range. The laser output was singly polarized with an average power of 2.7 mW.

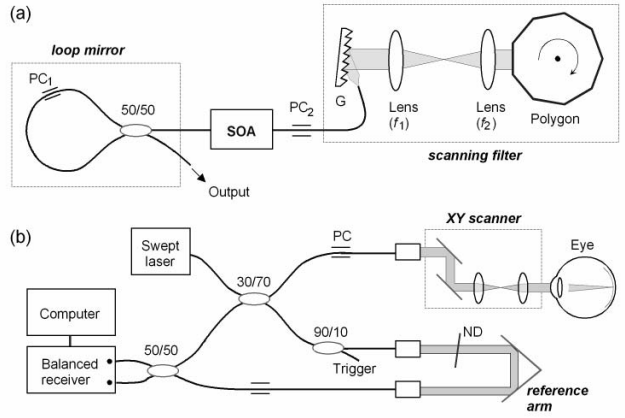

Fig. 1. Experimental setup: (a) wavelength-swept laser and (b) imaging system.

The output spectrum spanned from 1019 to 1081 nm over a range of 62 nm determined by the free spectral range of the filter. The spectral range coincided with a local transparent window of the eye. The roundtrip optical absorption in human vitreous and aqueous humors is estimated to be 3 - 4 dB based on known absorption characteristics of water [41]. Using a variable-delay Michelson interferometer, we measured the coherence length of the laser output, defined as the roundtrip delay resulting in 50% reduction in interference fringe visibility, to be approximately 4.4 mm in air. From this value, we calculated the instantaneous linewidth of laser output to be 0.11 nm. The oscilloscope trace of laser output showed a 100% tuning duty cycle at 18.8 kHz (single shot, 5-MHz detection bandwidth). When lasing was suppressed by blocking the intracavity beam in the polygon filter, the total power of amplified spontaneous emission (ASE) in the output was 0.5 mW. Since ASE is significantly suppressed during lasing, we expect that the ASE level in the laser output should be much lower. The laser output exhibited significant intensity fluctuations (~8%pp) due to an etalon effect originating from relatively large facet reflections at the SOA chip with a thickness equivalent to 2.5 mm in air. In the imaging system, the delayed optical waves by etalon reflection can cause ghost images; however, due to their relatively low magnitudes, we did not observe the artifacts in retinal imaging.

IMAGING SYSTEM

Using the swept laser as a light source, we constructed an OFDI system (Fig. 1(b)). The system further comprised a fiber-optic interferometer, a beam scanner, detection electronics and a computer. The sample arm (30% port) was connected to a human interface designed for retinal imaging [42]. The focal beam size was approximately 10 μm in tissue (index = 1.38). The optical power level at the entrance pupil of the eye was measured to be 550 μW, well below the 1.9-mW maximum exposure level at λ=1050 nm according to the ANSI laser safety standard for continuous exposure [43]. The reference arm (70% port) employed a transmission-type variable delay line and a 10% tap coupler to generate sampling trigger signals for data acquisition. A neutral-density (ND) attenuator was used to obtain the optimal reference-arm power. Light returning from the sample was combined with the reference light at a 50/50 coupler. Resulting interference signals were measured with an InGaAs dual-balanced detector (New Focus, Inc., 1811). The detector signal was further amplified (10 dB), low-pass filtered (DC to 5 MHz), and digitized at 10 MS/s with a 12-bit data acquisition board (National Instruments, Inc., PCI-6115). A total of 512 samples were acquired during each A-line scan. The imaging depth range determined by the spectral sampling interval was 2.44 mm in air.

RETINAL AND CHOROIDAL IMAGING

OFDI imaging was conducted with a healthy volunteer. The imaging system acquired a total 200,000 A-lines over 10.6 seconds as the focused sample beam was scanned over an area of 6 mm (horizontal) by 5.2 mm (vertical) across the macular region in the retina. Each image frame was constructed from a thousand A-line scans with an inverse grayscale table mapping to the reflectivity range (47 dB). Figure 2 depicts a typical frame showing the posterior segments of the volunteer's eye. The anatomical layers in the retina are clearly visualized and correlate well with previously published OCT images and histological findings. Figure 5(A) depicts an expanded image of fovea extracted from the three-dimensional data set. The OFDI image provides deep penetration into the choroid nearly up to the interface with the sclera, visualizing densely-packed choroidal capillaries and vessels.

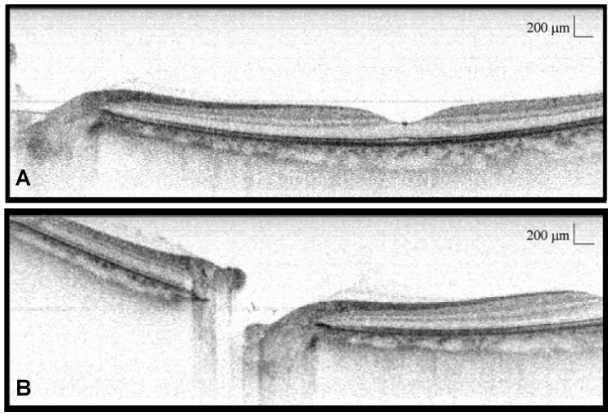

Fig. 2. OFDI images of human retina and choroid *in vivo* near the fovea (A) and optic head (B).

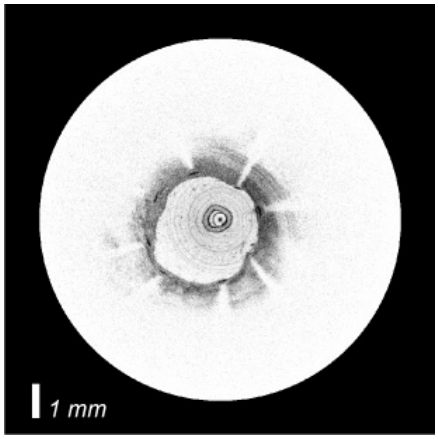

Fig. 3. OFDI image of a stented human coronary artery *ex vivo* acquired at 108 frames per second. The coronary stents are seen black in the image due to their high metallic reflectance.

CORONARY ARTERY IMAGING

We have also developed catheter-based OFDI systems for imaging coronary arteries and upper gastrointestinal tracts. To facilitate intravascular imaging, a 1.0 mm diameter, fiber-optic catheter and a rotary junction were fabricated. The rotary junction employed a high-speed DC motor for fast rotational scan. The catheter utilized a gradient index lens and 90-degree prism at its distal end and provided a transverse resolution of 25 μm. The rotary junction was mounted on a motorized linear translation stage to perform longitudinal, 3D pull-back imaging. The system employed a swept laser built in a 1250 – 1370 nm spectral range. Images of a fixed human coronary artery were acquired at 108 frames per second over the duration of 6 seconds as the catheter was rotated at 108 RPS and pulled back longitudinally at a speed of 7.2 mm/s. Figure 3 shows a typical OFDI image comprising 500 A-lines with 550 radial pixels.

CONCLUSIONS

Optical frequency domain imaging has emerged as a second generation technology for optical coherence tomography. With dramatically improved image acquisition speeds, OFDI holds great promise for a wide range of clinical diagnostic applications.

ACKNOWLEDGMENT

I thank the members of optical diagnostic group at the Wellman Center for Photomedicine for their technical contributions. This work was supported in part by the National Institute of Health through grants R33 CA110130, R01 HL076398, and R01 EY14975.

REFERENCES

[1] D. Huang, E. A. Swanson, C. P. Lin, J. S. Schuman, W. G. Stinson, W. Chang, M. R. Hee, T. Flotte, K. Gregory, C. A. Puliafito, and J. G. Fujimoto, "Optical coherence tomography," Science 254, 1178-1181 (1991).

[2] R. C. Youngquist, S. Carr, and D. E. N. Davies, "Optical coherence-domain reflectometry: A new optical evaluation technique," Opt. Lett., 12, 158-160 (1987).

[3] K. Takada, I. Yokohama, K. Chida, and J. Noda, "New measurement system for fault location in optical waveguide devices based on an interferometric technique," App. Opt. 26, 1603-1606 (1987).

[4] B. E. Bouma and G. J. Tearney, Handbook of optical coherence tomography (Marcel Dekker, New York, 2002).

[5] G. J. Tearney, M. E. Brezinski, B. E. Bouma, S. A. Boppart, C. Pitris, J. F. Southern, and J. G. Fujimoto, "In vivo endoscopic optical biopsy with optical coherence tomography," Science 276, 2037-2039 (1997).

[6] G. J. Tearney, B. E. Bouma, and J. G. Fujimoto, "High speed phase- and group-delay scanning with a grating based phase control delay line," Opt. Lett. 22, 1811-1813 (1997).

[7] M. Rollins, S. Yazdanfar, M. D. Kulkarni, R. Ung-Arunyawee, and J. A. Izatt, "In vivo video rate optical coherence tomography," Opt. Express 3, 219-229 (1998), http://www.opticsexpress.org/abstract.cfm?URI=OPEX-3-6-219

[8] J. M. Schmitt, "Optical coherence tomography (OCT): A review," IEEE J. Sel. Top. Quantum Electron. 5, 1205-1215 (1999).

[9] A. F. Fercher, C. K. Hitzenberger, G. Kamp, S. Y. El-Zaiat, "Measurement of intraocular distances by backscattering spectral interferometry," Opt. Commun. 117, 443-448 (1995).

[10] G. Hausler and M. W. Lindner, "Coherence Radar and Spectral Radar - new tools for dermatological diagnosis," J. Biomed. Opt. 3, 21-31 (1998).

[11] R. Leitgeb, C. K. Hitzenberger, and A. F. Fercher, "Performance of Fourier domain vs. time domain optical coherence tomography," Opt. Express 11, 889-894 (2003), http://www.opticsexpress.org/abstract.cfm?URI=OPEX-11-8-889

[12] J. F. de Boer, B. Cense, B. H. Park, M. C. Pierce, G. J. Tearney, and B. E. Bouma, "Improved signal-to-noise ratio in spectral-domain compared with time-domain optical coherence tomography," Opt. Lett. 28, 2067-2069 (2003).

[13] A. F. Fercher, W. Drexler, C. K. Hitzenberger, and T. Lasser, "Optical coherence tomography - principles and applications," Rep. Prog. Phys. 66, 239-303 (2003).

[14] S. R. Chinn, E. A. Swanson, and J. G. Fujimoto, "Optical coherence tomography using a frequency-tunable optical source," Opt. Lett. 22, 340-342 (1997).

[15] S. H. Yun, G. J. Tearney, J. F. de Boer, N. Iftimia, and B. E. Bouma, "High-speed optical frequency-domain imaging," Opt. Express 11, 2953-2963 (2003), http://www.opticsexpress.org/abstract.cfm?id=77825.

[16] W. Eickhoff and R. Ulrich, "Optical frequency domain reflectrometry in single-mode fiber", Appl. Phys. Lett. 39, 693-695 (1981).

[17] E. Brinkmeyer and R. Ulrich, "High-resolution OCDR in dispersive waveguide," Electron. Lett. 26, 413-414 (1990).

[18] W. V. Sorin, “Optical Reflectometry for component characterization” in Fiber optic test and measurement, D. Derickson, ed. (Prentice Hall PTR, New Jersey, 1998), pp. 383-433
[19] A. F. Fercher, C. K. Hitzenberger, G. Kamp, S. Y. El-Zaiat, “Measurement of intraocular distances by backscattering spectral interferometry,” Opt. Comm. 117, 43-48 (1995).
[20] F. Lexer, C. K. Hitzenberger, A. F. Fercher, and M. Kulhavy, “Wavelength-tuning interferometry of intraocular distances,” Appl. Opt. 36, 6548-6553 (1997).
[21] S. R. Chinn, E. Swanson, J. G. Fujimoto, “Optical coherence tomography using a frequency-tunable optical source,” Opt. Lett. 22, 340-342 (1997).
[22] B. Golubovic, B. E. Bouma, G. J. Tearney, and J. G. Fujimoto, “Optical frequency-domain reflectometry using rapid wavelength tuning of a Cr4+:forsterite laser,” Opt. Lett. 22, 1704-1706 (1997).
[23] U. H. P. Haberland, V. Blazek, and H. J. Schmitt, “Chirp optical coherence tomography of layered scattering media,” J. Biomed. Opt. 3, 259-266 (1998).
[24] M. A. Choma, M. V. Sarunic, C. H. Yang, and J. A. Izatt, "Sensitivity advantage of swept source and Fourier domain optical coherence tomography," Opt. Express 11, 2183-2189 (2003), http://www.opticsexpress.org/abstract.cfm?id=78787.
[25] S. H. Yun, G. J. Tearney, J. F. de Boer, M. Shishkov, W. Y. Oh, and B. E. Bouma, "Catheter-based optical frequency domain imaging at 36 frames per second," in *Coherence Domain Optical Methods and Optical Coherence Tomography in Biomedicine IX, 5690-16*(San Jose, CA, 2005).
[26] B. J. Vakoc, S. H. Yun, M. S. Shishkov, W. Oh, J. A. Evans, N. S. Nishioka, B. E. Bouma, and G. J. Tearney, "Comprehensive microscopy of the esophagus using optical frequency domain imaging," in *Coherence Domain Optical Methods and Optical Coherence Tomography in Biomedicine X, 6082-13*(San Jose, CA, 2006).
[27] R. Huber, M. Wojtkowski, J. G. Fujimoto, J. Y. Jiang, and A. E. Cable, "Three-dimensional and C-mode OCT imaging with a compact, frequency swept laser source at 1300 nm," Opt. Express 13, 10523-10538 (2005), http://www.opticsexpress.org/abstract.cfm?id=86656.
[28] Y. Yasuno, V. D. Madjarova, S. Makita, M. Akiba, A. Morosawa, C. Chong, T. Sakai, K. P. Chan, M. Itoh, and T. Yatagai, "Three-dimensional and high-speed swept-source optical coherence tomography for in vivo investigation of human anterior eye segments," Opt. Express 13, 10652-10664 (2005), http://www.opticsexpress.org/abstract.cfm?id=86669.
[29] J. Zhang, and Z. P. Chen, "In vivo blood flow imaging by a swept laser source based Fourier domain optical Doppler tomography," Opt. Express 13, 7449-7457 (2005), http://www.opticsexpress.org/abstract.cfm?id=85477.
[30] M. A. Choma, K. Hsu, and J. A. Izatt, "Swept source optical coherence tomography using an all-fiber 1300-nm ring laser source," J Biomed Opt 10, 44009 (2005).
[31] R. Huber, M. Wojtkowski, K. Taira, J. G. Fujimoto, and K. Hsu, "Amplified, frequency swept lasers for frequency domain reflectometry and OCT imaging: design and scaling principles," Opt. Express 13, 3513-3528 (2005), http://www.opticsexpress.org/abstract.cfm?id=83745.
[32] M. R. Hee, J. A. Izatt, E. A. Swanson, D. Huang, J. S. Schuman, C. P. Lin, C. A. Puliafito, and J. G. Fujimoto, "Optical Coherence Tomography of the Human Retina," Arch. Opthalmol. 113, 325-332 (1995).
[33] C. A. Puliafito, M. R. Hee, C. P. Lin, E. Reichel, J. S. Schuman, J. S. Duker, J. A. Izatt, E. A. Swanson, and J. G. Fujimoto, "Imaging of Macular Diseases with Optical Coherence Tomography," Ophthalmology 102, 217-229 (1995).
[34] A. Unterhuber, B. Povazay, B. Hermann, H. Sattmann, A. Chavez-Pirson, and W. Drexler, "In vivo retinal optical coherence tomography at 1040 nm-enhanced penetration into the choroid," Opt. Express 13, 3252-3258 (2005), http://www.opticsexpress.org/abstract.cfm?id=83715.
[35] S. Bourquin, A. D. Aguirre, I. Hartl, P. Hsiung, T. H. Ko, J. G. Fujimoto, T. A. Birks, W. J. Wadsworth, U. Bunting, and D. Kopf, "Ultrahigh resolution real time OCT imaging using a compact femtosecond Nd : Glass laser and nonlinear fiber," Opt. Express 11, 3290-3297 (2003), http://www.opticsexpress.org/abstract.cfm?id=78091.
[36] H. Lim, Y. Jiang, Y. M. Wang, Y. C. Huang, Z. P. Chen, and F. W. Wise, "Ultrahigh-resolution optical coherence tomography with a fiber laser source at 1 μm," Opt. Lett. 30, 1171-1173 (2005).
[37] M. Wojtkowski, R. Leitgeb, A. Kowalczyk, T. Bajraszewski, and A. F. Fercher, "In vivo human retinal imaging by Fourier domain optical coherence tomography," J. Biomed. Opt. 7, 457-463 (2002).
[38] N. A. Nassif, B. Cense, B. H. Park, M. C. Pierce, S. H. Yun, B. E. Bouma, G. J. Tearney, T. C. Chen, and J. F. de Boer, "In vivo high-resolution video-rate spectral-domain optical coherence tomography of the human retina and optic nerve," Opt. Express 12, 367-376 (2004), http://www.opticsexpress.org/abstract.cfm?id=78765.
[39] S. H. Yun, G. J. Tearney, J. F. de Boer, and B. E. Bouma, "Motion artifacts in optical coherence tomography with frequency-domain ranging," Opt. Express 12, 2977-2998 (2004), http://www.opticsexpress.org/abstract.cfm?id=80320.
[40] S. H. Yun, C. Boudoux, G. J. Tearney, and B. E. Bouma, “High-speed wavelength-swept semiconductor laser with a polygon-scanner-based wavelength filter,” Opt. Lett. 28, 1981-1983 (2003).
[41] D. J. Segelstein, The complex refractive index of water (University of Missouri-Kansas City, 1981).
[42] B. Cense, H. C. Chen, B. H. Park, M. C. Pierce, and J. F. de Boer, "In vivo birefringence and thickness measurements of the human retinal nerve fiber layer using polarization-sensitive optical coherence tomography," J. Biomed. Opt. 9, 121-125 (2004).
[43] American National Standards Institute, American national standard for safe use of lasers z136.1 (American National Standards Institute, Orlando, FL, 2000).